Proceedings of the 9ICEG
9th International Congress on Environmental Geotechnics
25-28 June, 2023 | Chania, Greece
© Authors: All rights reserved, 2023
https://doi.org/10.53243/ICEG2023-354

Hydration effects on the mechanical performance of GCLs looked through the lens of particle morphology

Gali Madhavi Latha[1], and Anjali G. Pillai[2]

[1]*Professor, Department of Civil Engineering, Indian Institute of Science Bangalore, Bengaluru-560012, India, email: madhavi@iisc.ac.in*

[2]*Ph.D. Student, Department of Civil Engineering, Indian Institute of Science Bangalore, Bengaluru-560012, India, email: anjalipillai@iisc.ac.in*

ABSTRACT

The present study brings out the role of particle shape on the hydration effects in GCLs through image-based particle shape characterizations, shear tests on sand-GCL interfaces and surface analysis of sheared GCLs. Two different sands with distinct particle shape, a rounded sand and an angular sand were chosen for the study with a wide variation in their shape parameters. Roundness, sphericity, and normalized roughness of the particles were quantified through digital imaging and MATLAB computations. Shear tests were carried out on sand-GCL interfaces in dry and saturated conditions under a wide normal stress range. It was observed that GCLs in contact with angular sands get less hydrated compared to the GCLs in contact with rounded sand because of the reduced permeability and increased tortuosity in angular sands. Image analysis of surfaces of exhumed GCL specimens revealed that the amount of sand trapped on the GCL surface varied with the particle shape, leading to the differences in their performance at large strains. The particle shape parameters, micro-scale kinematics at the interface and microscopic surface changes to the GCL surface are correlated to the macroscopic interface shear strength while understanding the hydration effects in GCL. The study highlights the importance of understanding the particle morphology in reducing the hydration effects in GCL while designing landfill systems.

Keywords: GCL, interface shear, particle morphology, digital image analysis, hydration effects

1 INTRODUCTION

Geosynthetic clay liners (GCLs) are perceived as an economical, superior, and sustainable alternative to the conventional clay liners in landfills. The self-healing capabilities, diffusive and advective resistance, easy installation procedures and low cost of GCLs made them an integral part of the liners and covers of many engineered landfills (Koerner & Daniel, 1995; Rowe, 2020). Consumption of GCLs has seen exponential growth in the past decade, which is evident through the global geosynthetic market trends. GCLs usually comprise a layer of bentonite sandwiched between two geotextiles, the carrier geotextile, and a cover geotextile. Whether they are used in liners or in covers, GCLs are in contact with soils. The composite GCL systems are invariably subjected to normal stresses and shear stresses, which can cause translational failures, if not effectively resisted through the soil-GCL interactions (Fox & Stark, 2015).

Another important factor that governs the mechanical response of GCLs is the hydration of bentonite core, whose primary role is to control the fluid transmission. During manufacturing, the GCLs gravimetric water contents of 5% to 40% are maintained in the bentonite layer (Acikel et al., 2018). After installation in a landfill, GCLs get hydrated by sucking water from the subgrade soils. This water hydrates the bentonite further and makes it swell, thus increasing the overall volume of the GCL. The swollen bentonite oozes out into the voids of the cover and carrier geotextiles and creates a slippery surface. The base and cover geotextiles in the GCL are connected through reinforcing fibres that penetrate through the bentonite layer, either by stitch- bonding or needle punching. These reinforcing fibres get ruptured due to fibre pull-out caused by swelling (Feng et al., 2020). These changes bring in entirely

new interaction mechanisms between the GCL and soil, affecting the overall interface shear response and resistance to sliding (Pillai & Gali, 2022a).

Recent studies suggest that the shear response of hydrated GCL interfaces is mainly governed by the water content in the bentonite layer, method of hydration, normal stress, and type of bentonite (Bradshaw & Benson, 2014; Bareither et al., 2018). Most of the available interface shear studies on GCLs are on geomembranes and geotextiles interfacing with GCLs. Studies on GCL-soil interfaces are not many. Very few of them are focused on particle morphology effects on the shear response of sand-GCL interfaces. With quick progression of high precision imaging techniques and computational abilities related to digital image analysis, some of the recent studies examined these aspects in detail (Pillai & Gali, 2022b). Understanding the effects of GCL hydration on the interface shear response through particle shape perspectives is a big challenge because of the multi-scale interlinked phenomena involved in the process. The current study provides a convenient method for such an analysis through precise particle shape quantifications, shear strength measurements of interfaces formed with GCL in contact with sand subgrade under varying conditions of hydration and surface change measurements of tested GCLs and relating all these aspects in the framework of particle morphology.

2 INTERFACE SHEAR TESTS

2.1 Test setup

A direct shear setup modified to conduct interface shear tests by replacing the bottom box with a rigid 180 mm square steel plate to which geosynthetic materials can be fixed was used for carrying out the interface shear tests in this study. A roller arrangement for the movement of plate along the direction of shear, lever arm arrangement for measuring the normal load, a horizontal load cell for measuring the shear load and an LVDT (linear variable differential transformer) for measuring the shear displacement complete the test setup. A photograph of the setup is shown in Figure 1.

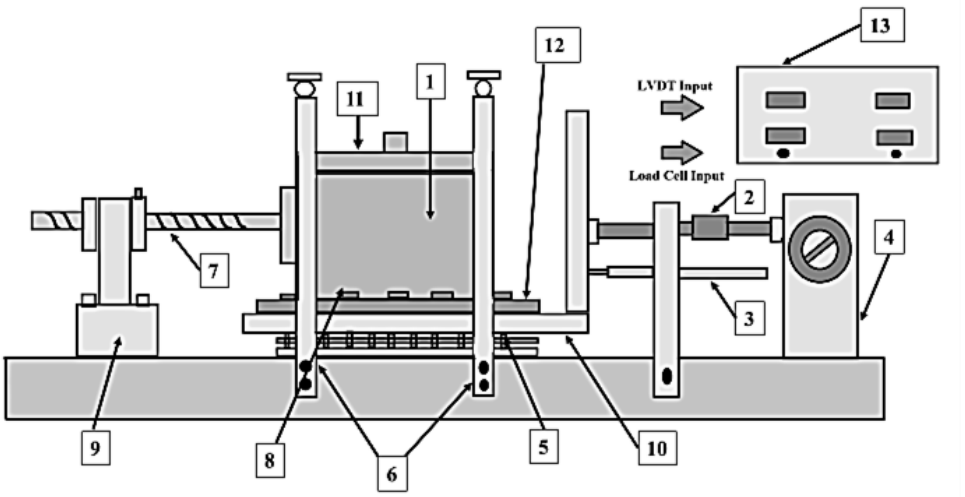

1) Sand in the shear box 2) horizontal load cell 3) LVDT 4) driving unit 5) rollers 6) holder plates 7) movable shaft 8) gripping clamps 9) tail stock 10) rigid steel plate 11) loading pad 12) GCL specimen 13) data logger

Figure 1. *Schematic diagram of the interface shear setup*

2.2 Test materials

The GCL used in this study has sodium bentonite core between a woven geotextile as the carrier layer and a needle-punched nonwoven geotextile as the cover layer, both made from polypropylene. Table 1 presents the properties of GCL, as given by the manufacturer. The sodium bentonite in the GCL has 70% montmorillonite and hence the layer has a high swelling capacity and high water absorption capacity.

Table 1. *Properties of GCL*

Property	Value
Mass per unit area (g/m^2)	4300
Average thickness (mm)	6
Montmorillonite content (%)	70
Swelling capacity (ml/2g)	24
Water absorption capacity (%)	650
Hydraulic conductivity (m/s)	5×10^{-11}
Tensile strength in machine direction (kN/m)	11.5

A natural sand (RS) collected from a riverbed and a manufactured sand (MS) obtained from stone crushing quarry were selected for this study to represent two different morphological conditions. Figure 2 presents the grain size distribution of the natural and manufactured sands. Originally the river sand was poorly graded, and the manufactured sand was well-graded. Their particle size ranges were also different, as seen in Figure 2. To eliminate the particle size and gradation effects, both the sand samples were scalped by choosing specific size fractions from these sands, to arrive at a common gradation for both the sands.

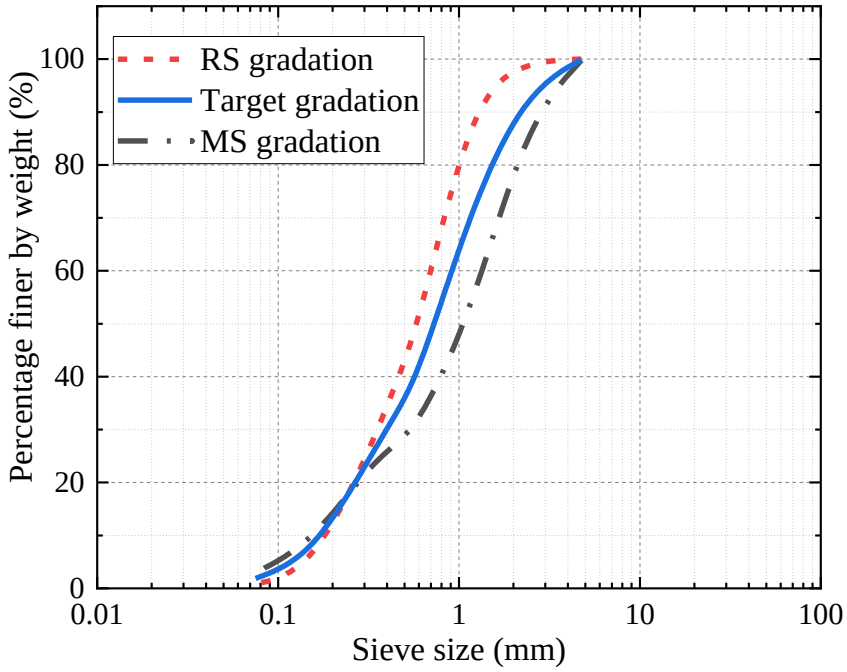

Figure 2. *Grain size distribution of original sands and chosen gradation for the current study*

Three different shape descriptors, namely, roundness, sphericity, and surface roughness were selected for the particle shape quantifications in this study. For obtaining these shape parameters, microscopic images of sand particles were procured in different orientations and shape parameters were analysed for these images using MATLAB algorithms written based on the following equations.

$$\text{Roundness (Wadell, 1935)} = \frac{\sum(\frac{r_i}{N_c})}{r_{max}} \quad (1)$$

$$\text{Sphericity (Wadell, 1932)} = \frac{D}{D_{cir}} \quad (2)$$

$$\text{Normalized Roughness (Vangla et al., 2018)} = \frac{1}{L}\sqrt{\frac{1}{N}\sum_{i=1}^{N}(y_{ir} - y_{is})^2} \quad (3)$$

where r_i is the radius of the circle that fits into the ith corner of the circle, N_c is the total number of the corners, and r_{max} is the maximum radius of circle that can be inscribed with the particle, D is the diameter of the circle which has the equivalent projected area of the particle, D_{cir} is the minimum diameter of the

circle that circumscribes the particle, N is the number of roughness measurements, y_{ir} and y_{is} are the ith coordinates of the raw profile and the smoothened profile, respectively and L is the length of the particle.

From each sand sample, 200 particles were randomly taken from each size fractions of 0.075 mm, 0.15 mm, 0.3 mm and 0.6 mm. Microscopic images in two different orientations were obtained for these particles through an optical microscope. Digital images of typical sand particles are shown in Figure 3. These digital images were converted to binary images in MATLAB and the binary images were analysed in MATLAB for obtaining their shape parameters. Morphological parameters of all these particles were determined through MATLAB algorithms developed for Equations (1)-(4). Average morphological parameters for river sand and manufactured sand particles computed for different size ranges are given in Table 2. As seen from the data, river sand particles have higher roundness and sphericity compared to quarry sand because of the natural erosion process that would have occurred during its deposition. This means that natural sand particles have a shape closer to that of a sphere and smooth corners, as can be visualized from Figure 3. Manufactured particles have lesser roundness, sphericity, and higher roughness, because of the irregular cutting that happens during stone crushing. Hence their shape is elongated, and their corners are irregular. Roughness, which is a measure of the microscopic irregularities on the surface, is much higher for manufactured sand particles compared to that of the natural sand particles, implying that MS particles generate higher friction when they are in contact with neighbouring particles or with polymeric interfaces.



Figure 3. *Microscopic images of typical sand particles: River sand (left) Manufactured sand (right)*

Table 2. *Morphological properties of sands*

Sand Type	Particle size (mm)	Roundness	Sphericity	Roughness (normalized)
RS	0.6000	0.4001	0.8155	0.0010
RS	0.3000	0.3818	0.8207	0.0009
RS	0.1500	0.4556	0.8689	0.0008
RS	0.0750	0.4340	0.8842	0.0021
MS	0.6000	0.3898	0.7708	0.0024
MS	0.3000	0.3740	0.7817	0.0015
MS	0.1500	0.4017	0.7912	0.0009
MS	0.0750	0.3971	0.8003	0.0050

2.3 Testing procedure

Specimens of GCL cut to a size of 180 mm square were clamped to the rigid steel base. The upper box was then placed above the GCL specimen and filled with sand and compacted to a relative density of 80%. To achieve this, quantity of sand required for the given volume of the shear box was computed and it was divided into 3 portions, each portion placed in the shear box sequentially and compacted with a wooden rod with rubber base to achieve one third of the total volume. Shearing rate used in the tests was 1.0 mm/min. Normal stresses of 7, 15, 30, 60 and 100 kPa were used in the tests with dry sand. Tests were carried out in dry and saturated conditions of sand with a dry GCL layer placed above it. Required water content in sand for complete saturated was computed as 18%. In saturated tests, adequate waiting time was allowed after preparing the specimen, to achieve equilibrium water content of the GCL specimen. Saturated tests were carried out at normal stresses of 7 kPa and 100 kPa. The lower normal stress of 7 kPa represents the case of sand-GCL interfaces in cover systems and the higher normal stress of 100 kPa represents the case of sand-GCL interfaces in liner systems. In all interface shear tests, woven geotextile surface was in contact with the sand. Table 3 gives the test matrix used for the present study. The first letter of the test code denotes the sand type followed by a number that denotes the normal stress, the following letter *w* represents water content followed by the

percentage of water content given as a number. The test code R100w0 for example represents the test with river sand conducted at a normal stress of 100 kPa with dry sand.

Table 3. *Test Matrix*

Test code	Sand Type	Interface	Normal stress (kPa)	Water content in sand (*w*) (%)
R7w0	RS	GCL-RS	7	0
R7w18	RS	GCL-RS	7	18
R100w0	RS	GCL-RS	100	0
R100w18	RS	GCL-RS	100	18
M7w0	MS	GCL-MS	7	0
M7w18	MS	GCL-MS	7	18
M100w0	MS	GCL-MS	100	0
M100w18	MS	GCL-MS	100	18

3 RESULTS AND DISCUSSION

3.1 Dry Interface Shear Tests

Results of interface shear tests on sand-GCL interfaces under dry conditions are shown in Figure 4. Shear response of river sand and manufactured sand is compared at normal stresses of 7 kPa and 100 kPa, respectively in Figure 4a and Figure 4b. At both the normal stresses, manufactured sand showed higher shear resistance compared to river sand because of the angularity of sand particles. Within the experimental displacement limits, peak shear stress was attained in case of low normal stress of 7 kPa, but the response at 100 kPa was observed to be still in strain-hardening stage, without a peak. However, the difference in shear stress observed at any specific displacement stage was higher for manufactured sand at both the normal stresses. The reason for the difference in response is the difference in the interactions between sand particles and geosynthetic surface. While rounded RS particles roll and slide easily along the interface, angular MS particles offer resistance to rolling and sliding because of their shape and they get interlocked at the interface, causing higher resistance to move them along the interface.

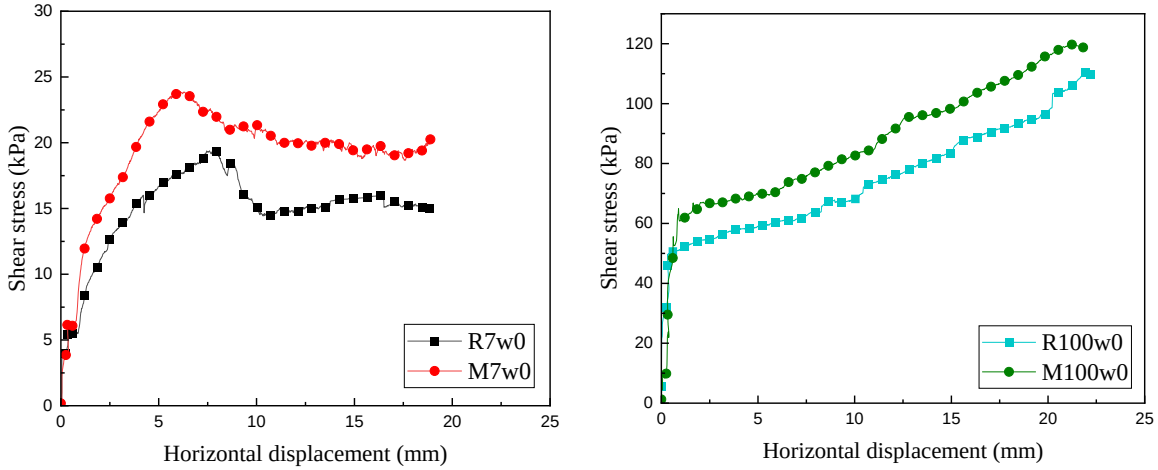

Figure 4. *Shear response of dry interfaces at different normal stresses: Normal stress of 7 kPa (left). Normal stress of 100 kPa (right)*

3.2 Wet Interface Shear Tests

Results of interface shear tests on sand-GCL interfaces under saturated conditions are shown in Figure 5. Interface shear response of saturated river sand and saturated manufactured sand is compared at normal stresses of 7 kPa and 100 kPa, respectively in Figure 5a and Figure 5b. Comparison of Figure

4 and Figure 5 reveals that the interface shear resistance considerably decreased with the hydration for both the interfaces. At a normal stress of 7 kPa, the peak shear stress reduced by 5 kPa for both river sand and manufactured sand interfaces. At 100 kPa, peak shear stress reduced by 28 kPa for river sand interface and 24 kPa for manufactured sand interface. Reason for the reduction in shear resistance is the lubricating effect of the bentonite which got extruded through the pores of the geotextile, forming a slippery layer at the shearing plane. The extruded bentonite forms a slippery layer around the sand particles, causing reduction in sand particle friction, thus contributing further to the reduction in overall shear resistance. With increase in normal stress, the GCL is squeezed more, extruding a larger amount of wet bentonite on to the shearing plane. Thus, the reduction in shear resistance with saturation is higher at higher normal stresses. When RS and MS are compared for their performance in interface shear under saturated conditions, reduction in shear resistance with saturation is relatively lower in case of manufactured sand because of the lower permeability and higher tortuosity offered by the irregular shaped MS particles.

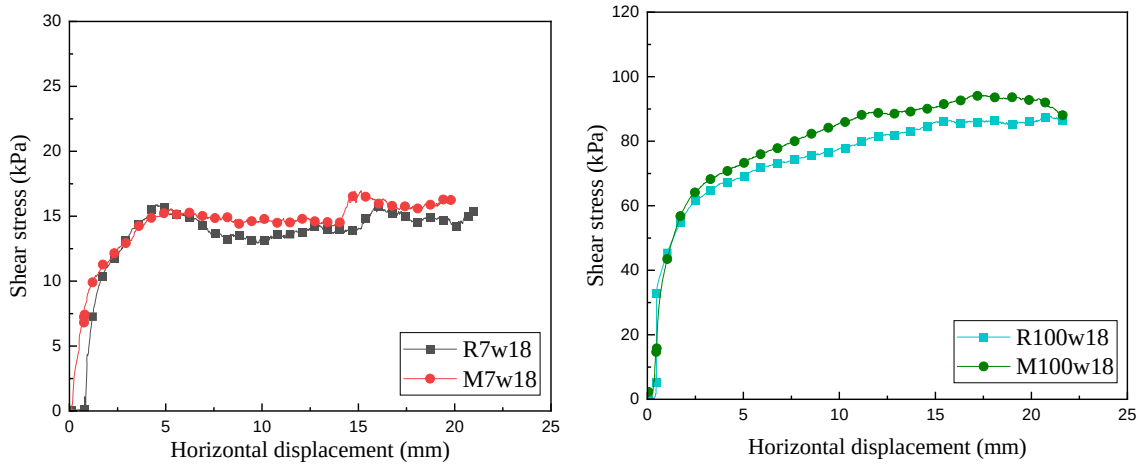

Figure 5. *Shear response of wet interfaces at different normal stresses: Normal stress of 7 kPa (left). Normal stress of 100 kPa (right)*

3.3 Digital Image Analysis

GCL surfaces before and after the interface shear tests were examined through high resolution images captured through a HD Camera. A rectangular surface measuring 12 cm × 10 cm cut from the central portion of the GCL was analysed in small square segments of 2 cm × 2 cm and the images were stitched together to get best possible resolution of the images. The individual segments converted into binary images using MATLAB 2021a and analysed for surface features. Figure 6 shows the photographs of the surfaces of untested and tested GCLs and Figure 7 shows the corresponding binary images generated by MATLAB



Figure 6. *Photographic images of GCL surfaces: Untested (left). Tested with RS (middle). Tested with MS (right)*

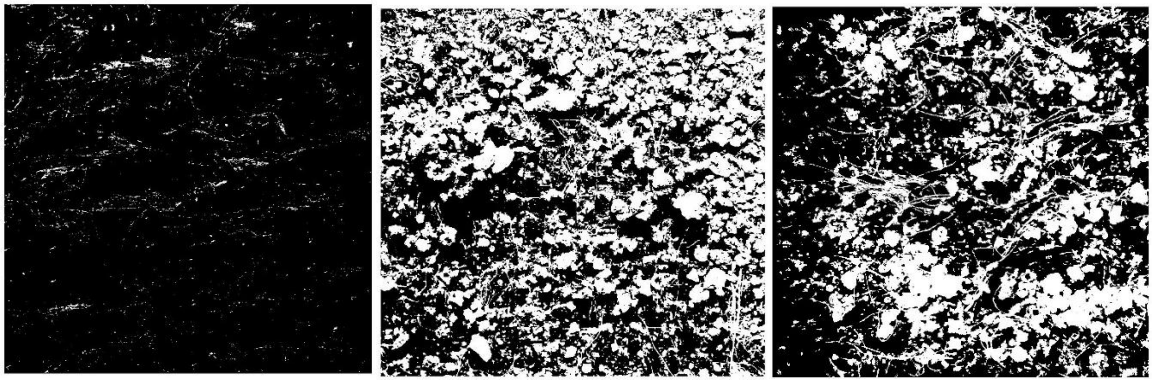

Figure 7. *Binary images of GCL surfaces: Untested (left). Tested with RS (middle). Tested with MS (right)*

The inbuilt region properties function of MATLAB was used for analysing the binary images. As observed from Figure 7, GCL surfaces had entrapped sand particles after interface shear tests, indicated by white spots in the binary images. The density of these spots is higher in case of RS, indicating that sand particle entrapment is higher for RS interfaces. Using the region properties function, the density of white spots was calculated, which corresponds to the area covered by the sand grains after the interface shear test. Table 4 presents the results from image analysis of GCL surfaces.

Table 4. *Test Matrix*

Test code	Sand Type	Normal stress (kPa)	Water content in soil (*w*) (%)	Area of sand entrapment (%)
R7w0	RS	7	0	1.85
R7w18	RS	7	18	25.45
R100w0	RS	100	0	3.20
R100w18	RS	100	18	38.30
M7w0	MS	7	0	1.41
M7w18	MS	7	18	20.37
M100w0	MS	100	0	2.69
M100w18	MS	100	18	25.82

Under dry conditions, area of sand entrapment was comparable for GCLs tested with RS and MS at both the normal stresses. Higher entrapment at higher normal stress can be easily explained through the increase in pressure that pushed the particles into the voids of the woven geotextile surface. Further, Table 4 shows substantial increase in sand particle entrapment under wet conditions, the increase more pronounced in case of RS. The extruded bentonite present at the interface helped in getting more sand particles getting stuck into the void spaces of the geotextile. Since the effects of saturation are relatively less in case of MS, the area of sand particle coverage was also less in MS at both normal stresses.

The results of direct shear tests on sand-GCL interfaces under dry and saturated conditions followed by MATLAB analysis of surface changes to GCL clearly provided microscopic clues to the macroscopic interface shear response of these interfaces. Since sand particles in manufactured sand (MS) are angular and irregular, GCLs interfacing with MS showed highest resistance to shear compared to those interfacing with rounded particles in river sand (RS). Saturation caused reduction in shear resistance due to dual action of bentonite extrusion that causes slippages at the interface and reduction in intergranular friction. The effects of saturation are less in case of irregular particles in manufactured sand because of interlocked grains that result in lower permeability and higher tortuosity. The irregular elongated shape of particles in manufactured sand is also found to be beneficial for reducing the entrapment of sand grains on to the voids of the geotextile, thereby hampering the reduction in shear resistance. Overall, GCL interfaces with manufactured sand showed higher interface shear strength under dry and saturated conditions, proving their better performance against translational failures due

to inadequate interface shear resistance. These findings demonstrate that manufactured sand can be a sustainable and effective alternative for river sand in the construction of engineered landfills.

4 CONCLUSIONS

The following major conclusions are drawn from this study.

1. Compared to rounded river sand particles, angular manufactured sand particles provide higher interface shear resistance due to their elongated shape and irregular and rough surface.
2. Saturation reduces the interface shear resistance drastically because of sticky bentonite extrusion that causes lubrication and increases the sand grain entrapment into the voids of the geotextile.
3. Effects of sand saturation are higher in case of river sand because of its higher permeability and lower tortuosity. The difference in peak shear stress under dry and saturated conditions is 5 kPa for RS and MS at a lower normal stress of 7 kPa and 24 and 28 kPa, respectively, for MS and RS at a higher normal stress of 100 kPa.
4. Digital image analysis of GCL surfaces before and after the shear tests helped in quantification of area of sand particle entrapment, which is higher in case of RS compared to MS, leading to further reduction in the interface shear resistance.
5. This study demonstrated that manufactured sand can be a sustainable and effective alternative for river sand in the construction of engineered landfills.

5 ACKNOWLEDGEMENTS

Authors thank M/s Maccaferri Environmental Solutions Pvt. Ltd. for providing the GCLs and the SERB of Department of Science and Technology, India for granting the POWER Fellowship to the corresponding author, through which the experiments were supported.

REFERENCES

Acikel, A. S., Gates, W. P., Singh, R. M., Bouazza, A. & Rowe, R. K. (2018). Insufficient initial hydration of GCLs from some subgrades: Factors and causes, Geotextiles and Geomembranes, 46(6), 770-781.

Bareither, C. A., Soleimanian, M. R., & Ghazizadeh, S. (2018). Direct shear testing of GCLs at elevated temperature and in a non-standard solution. Geosynthetics International, 25 (3), 350-368.

Bradshaw, S. L., & Benson, C. H. (2014). Effect of municipal solid waste leachate on hydraulic conductivity and exchange complex of geosynthetic clay liners. Geotechnical and Geoenvironmental Engineering, 140(4), 04013038.

Feng, S., Chang, J., Chen, H., Shen, Y., & Shi, J. (2020). Shear strength and failure mechanism of needle-punched geosynthetic clay liner, Geotextiles and Geomembranes, 48(6), 962-972.

Fox, P. J., & Stark, T. D. (2015) State-of-the-art report: GCL shear strength and its measurement – ten-year update. Geosynthetics International, 22, 3–47.

Koerner, R.M., & Daniel, D.E. (1995). A suggested methodology for assessing the technical equivalency of GCLs to CCLs. In R.M. Koerner, E. Gartung, & H. Zanzinger (Ed.), Geosynthetic clay liners, (pp. 73–98). A.A. Balkema, Rotterdam.

Pillai, A. G., & Gali, M. L. (2022a). New perspectives on bentonite hydration and shear strength of GCL-sand interfaces based on particle shape characterizations. International Journal of Geosynthetics and Ground Engineering, 8, 25.

Pillai, A., & Latha G. M. (2022b). Role of particle shape on the shear strength of sand-GCL interfaces under dry and wet conditions. Geotextiles and Geomembranes, 50 (2), 262-281.

Rowe, R. K. (2020). Geosynthetic clay liners: perceptions and misconceptions. Geotextiles and Geomembranes, 48(2), 137–156.

Vangla, P., Roy, N., & Gali, M. L., (2018). Image based shape characterization of granular materials and its effect on kinematics of particle motion. Granular Matter, 20(1), 1-19.

Wadell, H. (1932). Volume, shape, and roundness of rock particles. The Journal of Geology, 40(5), 443-451.

Wadell, H. (1935). Volume, shape, and roundness of quartz particles. The Journal of Geology, 43(3), 250-280.